



HAL
open science

Greening effect of slag cement-based concrete: Environmental and ecotoxicological impact

Julien Couvidat, Cécile Diliberto, Eric Meux, Sylvie Cotelle, Clement Bojic,
Laurent Izoret, André Lecomte

► To cite this version:

Julien Couvidat, Cécile Diliberto, Eric Meux, Sylvie Cotelle, Clement Bojic, et al.. Greening effect of slag cement-based concrete: Environmental and ecotoxicological impact. Environmental Technology and Innovation, 2021, 22, pp.101467. 10.1016/j.eti.2021.101467 . hal-03291838

HAL Id: hal-03291838

<https://hal.science/hal-03291838>

Submitted on 22 Mar 2023

HAL is a multi-disciplinary open access archive for the deposit and dissemination of scientific research documents, whether they are published or not. The documents may come from teaching and research institutions in France or abroad, or from public or private research centers.

L'archive ouverte pluridisciplinaire **HAL**, est destinée au dépôt et à la diffusion de documents scientifiques de niveau recherche, publiés ou non, émanant des établissements d'enseignement et de recherche français ou étrangers, des laboratoires publics ou privés.



Distributed under a Creative Commons Attribution - NonCommercial 4.0 International License

1 Greening effect of slag cement-based concrete: environmental and 2 ecotoxicological impact

3 Julien Couvidat ^{a,*,i}, Cécile Diliberto ^a, Eric Meux ^b, Sylvie Cotelle ^c, Clement Bojic ^c,
4 Laurent Izoret ^d, André Lecomte ^a

5 ^a Université de Lorraine, CNRS, IJL, F-54000 Nancy, France

6 ^b Université de Lorraine, CNRS, IJL, F-57000 Metz, France

7 ^c Université de Lorraine, CNRS, LIEC, F-57000 Metz, France

8 ^d Technical Association of the French Cement Industry (ATILH), F-92974 Paris-La-Défense
9 Cedex, France

10 * Address correspondence to Julien Couvidat, julien.couvidat@insa-lyon.fr, +33 (0)6 66 70 36
11 05 (France)

12 **Data accessibility statement**

13 Data pertaining to this manuscript are deposited in figshare at DOI:

14 10.6084/m9.figshare.13049582

15 **Highlights**

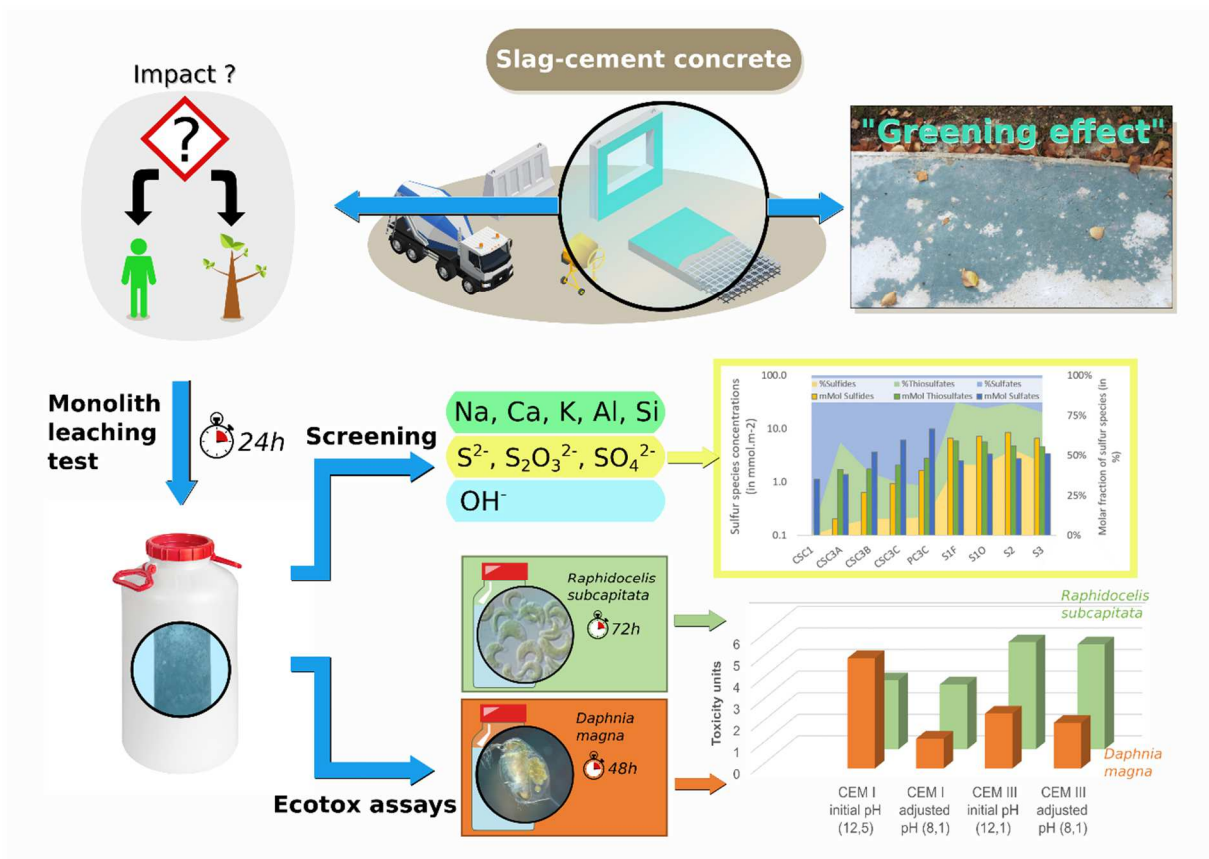
- 16 - Greening effect is not associated with hazardous leachates or ecotoxic effects
- 17 - Alkaline pH (> 11) is the main issue with cement or slag-based materials
- 18 - The algae *R. subcapitata* is not affected by high pH unlike the crustacean *D. magna*
- 19 - GBFS contain sulfides up to 1 wt.% release in eluates of concretes and pastes
- 20 - Sulfides are quickly neutralized in natural environment

ⁱ Present address: Univ Lyon, INSA Lyon, DEEP, EA7429, 69621 Villeurbanne, France

21 **Abstract**

22 Materials containing ground granulated blast furnace slag (GGBFS) display a transient green-
23 blue color after demolding. This greening effect have been investigated for leaching behavior
24 and ecotoxicological impact. Color of concretes and pure pastes containing GGBFS was
25 assessed with a portable spectrophotometer, and samples were then submitted to a tank
26 monolith leaching test. Ecotoxicological tests were conducted on reference sample and a
27 green concrete sample at both natural and adjusted pH of 8.1. Main results support that the
28 temporary greening effect of GGBFS-containing materials has no particular impact neither on
29 the chemistry of leachates, nor ecotoxicity. Additionally, alkaline leachates are the main issue
30 of leached cement or GGBFS based materials with pH around 11.5 – 12.5. Alkaline pH is a
31 preponderant factor of ecotoxicity to sensitive organisms such as *Daphnia magna*,
32 immobilization assay (48h) resulting in 5.10 Toxic Units (TU) for reference sample at pH
33 12.50 against 1.38 TU at pH 8.10. Furthermore, sulfides are a specific issue of GGBFS
34 materials concentrated up to 0.94 mmol.m⁻² in leachates, having an ecotoxic impact on living
35 organisms at all trophic levels. At pH 8.10, green concrete leachates have 4.85 TU for
36 *Raphidocelis subcapitata* growth assay (sulfides concentration of 0.63 mmol.m⁻²) against 3.0
37 TU for green concrete sample. However, sulfides are easily removed from natural solution by
38 oxidation or evaporation.

39



40

41 **Graphical abstract (color on web only):** Green slag cement-based concrete releases cations
 42 and sulfur anions, including sulfides, associated to a very low ecotoxic effect.

43 **Keywords:** blast-furnace slag, greening effect, sulfides, cement, ecotoxicological assay,
 44 leaching test

45

46 1. Introduction

47 Granulated Blast Furnace Slag (GBFS) is generated during iron production, as a by-product,
48 solidified by high-pressure water quenching. In 2019, about 371 Mt of blast furnace slag
49 (BFS) have been produced worldwide (including GBFS, but also air-cooled, expanded, and
50 pelletized), against 227 Mt in 2000 (Worldsteel Association 2020). Quenching of molten slag
51 develops interesting properties, among which a vitreous structure allowing GBFS to be used
52 as a Supplementary Cementitious Material (SCM) in civil engineering, combined to clinker in
53 composite cements. GBFS is a sought-after SCM for its mechanical and durability properties
54 in aggressive environment.

55 Hydrated and activated Ground GBFS (GGBFS) depicts a noticeable blue-green coloration
56 after form removal, either with clinker or not. This transient phenomenon, called “greening
57 effect”, disappears in days to weeks following the contact with air. Widely known from public
58 workers, builders, or civil engineers, the greening effect has long been ignored in the research
59 field until recently. Diverse hypothesis have been discussed in literature on the origin of the
60 coloration, mostly involving iron compounds (Mansfeldt and Dohrmann 2001; Sioulas and
61 Sanjayan 2001; Schwab et al. 2006), and sulfides (Vernet 1982). This latter hypothesis has
62 been consolidated by a recent study using UV-visible-near infrared Diffuse Reflectance
63 spectroscopy (Le Cornec et al. 2017). Le Cornec’s main findings sustain a mechanism of
64 coloration involving optical transitions due to ionic sulfides radicals. Such chromophore
65 species, $S^{2\cdot-}$ and $S^{3\cdot-}$, rather unusual, are well known in gemology to be responsible of the blue
66 color of the semi-precious stone Lapis Lazulis (Steudel 2003; Chivers and Elder 2013). In the
67 case of GGBFS-containing materials, it is most likely that these species are formed during
68 early hydration, and trapped by solid solution of sulfides in aluminates hydrates (Vernet 1982;
69 Le Cornec et al. 2017).

70 However, despite the widely known greening effect phenomenon, in tune with the use of
71 GGBFS in local small constructions and in more important work, the transient vivid color has
72 long been of minor concern in the research field. For operator's safety and environmental
73 considerations, users of composite cements (CEM III type cements) have started asking
74 questions over time to the cement industry about the environmental and health impact of
75 colored GGBFS-containing materials. Some studies have focused on the global environmental
76 impact of slags (Piatak et al. 2015), but none have focused on the potential effect of this
77 transitory coloration. More generally, leaching tests have been used in the construction
78 materials field to evaluate multiple environmental and geochemical aspects, such as diffusion
79 and transport mechanisms or short and long-term leaching of hazardous substances (Hillier et
80 al. 1999; Haga et al. 2005; Kamali et al. 2008; Müllauer et al. 2015; Märkl et al. 2017; Parron-
81 Rubio et al. 2019).

82 Besides classical physicochemical screening of known compounds in eluates, ecotoxicity
83 assessment allows the determination of a potential total toxicity of bioavailable
84 substances/materials towards living organisms. However, not much researches have been
85 conducted on classical construction materials, such as ordinary Portland cement, or GBFS
86 (Kobetičová and Černý 2017). The green microalgae *Raphidocelis subcapitata* and the
87 freshwater microcrustacean *Daphnia magna* are extensively used in aquatic toxicology
88 studies (Lapa et al. 2007; Choi et al. 2013; Rodrigues et al. 2020). The bioassays performed
89 using these species frequently follow international guidelines for chemicals. To determine the
90 acute toxicity of a given chemical, the population growth rate of *R. subcapitata* and the
91 mobility of *D. magna* are assessed according to the international standardized protocols ISO
92 8692 (2012) and ISO 6341 (2012), respectively.

93 A mixed approach involving chemical screening and ecotoxicological assessment has been
94 recently emphasized towards construction products as more efficient to identify non-specific

95 effects of possible hazardous substances (Bandow et al. 2018). The ecotoxicological
96 assessment of construction materials will be soon normalized by a coming European standard
97 (draft standard “Construction Products - Assessment of release of dangerous substances –
98 Determination of ecotoxicity of construction product eluates” FprCEN/TS, 2019).

99 The goal of the present study is to assess the environmental impact of the greening effect in
100 GGBFS-containing materials (e.g. mortar or concrete) subjected to a leaching contact with
101 water through a well-known standardized single-batch leaching test on solidified monolith.
102 Two research axes are followed: i) an assessment of the physicochemical composition of
103 leachates, followed by ii) an ecotoxicological evaluation of selected leachates with
104 appropriate tests. *Daphnia magna* has been selected regarding its recognized sensitivity (Lapa
105 et al. 2007; Rodrigues et al. 2020), combined with *Raphidocelis subcapitata* to assess a
106 different trophic level. Since pH of leachates might be out of the living range of the organisms
107 used, both ecotoxicological assays will be conducted with natural and adjusted pH
108 (Kobetičová and Černý 2017).

109 2. Materials and methods

110 2.1. Materials of the study

111 Concretes and cement pastes were formulated with four industrial cements (CEM I and CEM
112 III), and pure GGBFS pastes with three pure GGBFS of distinct origins directly obtained from
113 producers. Cements were used to make one cement paste and concretes, with aggregates, and
114 GGBFS were used to make pure pastes. The studied samples contained a variable amount of
115 GGBFS, from 0% to 100%. The 0% sample was a concrete made with CEM I cement, used as
116 a comparison reference. CEM I cement is mainly produced with clinker, gypsum and possibly
117 some minor additions up to 5 wt.% and contains no GGBFS. Three commercially available

118 CEM III cements were used, mainly constituted from GGBFS, clinker and gypsum or
 119 anhydrite, the class of which depends on the amount of GGBFS incorporated: CEM III/A
 120 contains between 36 and 65% of GGBFS, CEM III/B between 66 and 80% of GGBFS, and
 121 CEM III/C between 81% and 95% of GGBFS. The three pure GGBFS come from 3 different
 122 blast furnaces (named “S1”, “S2”, and “S3”), with two S1 GGBFS used, one from a fresh
 123 production (<2 months) and named “S1F”, and a second from an older production in stock
 124 (around 3 years) named “S1O”.

125 The fineness of cements and GGBFS, given as Blaine specific surface area, was not modified
 126 and ranged between 3600 and 5400 cm².g⁻¹ for the four cements, and between 4000 and 4815
 127 cm².g⁻¹ for the four GGBFS. The BFS of fresh production was received as a sand 0/2 and and
 128 was ground with a ring mill to about 4000 cm².g⁻¹. All data concerning the materials used in
 129 the present study are gathered in **Table 1**.

130 **Table 1.** Composition of cements and GGBFS used as hydraulic binder for concretes and pure
 131 pastes preparation.

Materials	GBFS wt.%	S ²⁻ g(S)/100g	Al ₂ O ₃	CaO	Fe ₂ O ₃	K ₂ O	MgO wt.%	MnO	Na ₂ O	SiO ₂	SO ₃
CEM I	0	-	5.44	62.91	3.03	0.81	1.89	0.08	0.20	20.69	3.33
CEM III/A	62	0.61	9.91	48.91	1.84	0.55	4.64	0.39	0.35	29.74	2.72
CEM III/B	71	0.55	9.56	47.62	1.15	0.55	4.99	0.24	0.22	31.32	3.52
CEM III/C	85	0.74	10.54	44.87	0.79	0.34	5.80	0.28	0.31	33.74	3.00
S1F	100	0.84	11.42	41.81	0.74	0.37	6.90	0.30	0.24	37.37	1.47
S1O	100	0.84	11.40	41.65	0.62	0.38	6.97	0.42	0.22	37.29	1.53
S2	100	0.79	11.89	41.49	0.35	0.41	7.16	0.29	0.27	37.57	0.86
S3	100	0.76	11.20	42.41	0.40	0.50	6.63	0.27	0.33	37.28	1.22

132

133 Description: Composition of CEM I, CEM III/A, CEM III/B, CEM III/C cements, and S1F
 134 (fresh production of S1), S1O (stock production of S1), S2 and S3 GGBFS is given in this
 135 table. GGBFS content is given as wt.%, sulfides content is given as g of sulfur for 100 g of
 136 binder, and major elements are given as oxides in wt.%.

137 Concretes were formulated with cement and a siliceous alluvial aggregate (from Moselle
138 river), commonly employed for concrete preparation in the North-East of France. A cement
139 paste was formulated only with the CEM III/C cement, which have the highest GGBFS
140 content of CEM III type cements according to EN 197-1. Pure pastes of GGBFS were made
141 with a mix of several productions of a same production site, water and 5% w/w of NaOH as
142 activator of the hydraulic setting.

143 Cements and GGBFS major composition was established by X-Ray Fluorescence (XRF) with
144 a Bruker S4 Explorer spectrometer, on fused beads. Data were recovered and processed with
145 the SpectraPlus software (Table 1).

146 GGBFS has usually noticeable amounts of sulfur, usually between 0.2 and 3.5 wt.%, mostly
147 under reduced form (Glasser et al. 1988; Piatak et al. 2015). Thus, sulfides are quantified in
148 GGBFS-containing cements and pure GGBFS powders, accordingly to the French cement
149 standard (NF EN 196-2, 2013) through an acid distillation and subsequent recovery of H₂S in
150 an alkaline solution. Regarding to the standard, some modifications were made: an alkaline
151 buffer solution called Sulfides Anti-Oxidant Buffer (SAOB) was used as recovery solution,
152 allowing analysis with an ion-selective electrode. The SAOB solution was prepared with 67 g
153 of Ethylenediaminetetraacetic acid (EDTA), 35 g of ascorbic acid and 80 g of NaOH for one
154 liter. A bubble jar filled with the SAOB solution was connected to the outlet of the distillation
155 apparatus to recover the gases. At the end, the SAOB solution was analyzed with an ion-
156 selective electrode Thermo Scientific Orion Silver/Sulfide 9616BNWP plugged on an HP
157 multimeter (model 3478A). The electrode calibration was achieved with serial dilutions of a
158 sulfide stock solution. Dilutions were prepared daily from a 1000 mg.L⁻¹ Mettler Toledo
159 sulfide ISE standard, formerly standardized with an AgNO₃ solution. Silver calibration
160 solution was beforehand calibrated with a KCl solution. All calibrations were made using the
161 silver/sulfide electrode on a Tacussel TT-Processeur 2 automated titrator.

162 2.2. *Concrete, cement and GGBFS paste preparation and conditioning*

163 A Controlab Perrier concrete mixer was used for the preparation of concretes and of cement
164 and GGBFS pastes. The water-to-binder ratio was kept to 0.5 for all preparations. Concretes
165 were prepared according to the following formula: 885 kg.m⁻³ of 0–5 mm sand, and 750 kg.m⁻³
166 of 4–8 mm gravel, 210 kg.m⁻³ of water and 420 kg.m⁻³ of cement. Concrete samples were
167 named “CSC1” for Concrete Sample with CEM I cement, “CSC3A” for CEM III/A based
168 concrete, “CSC3B” for CEM III/B based concrete and “CSC3C” for CEM III/C based
169 concrete. The cement paste was only made up with water and CEM III/C cement, to keep the
170 water-to-binder ratio to 0.5, and is named “PC3C”. The GGBFS pure pastes were made of
171 GGBFS mixed with water with a water-to-binder ratio of 0.5, activated by NaOH with an
172 activator-to-binder ratio of 5 wt.%. GGBFS pastes were named accordingly with previous
173 denomination, i.e. “S1F” and “S1O” for fresh and old production of S1 GGBFS, “S2”, and
174 “S3” for the two others GGBFS used.

175 All compounds were mixed following the NF EN 196-3 (09/2017) standard for cement and
176 GGBFS pastes, and the NF EN 196-1 (09/2016) standard for concrete samples. Cylindrical
177 high density polyethylene (HDPE) bottles (7.2 cm diameter, 12.5 cm height) were used as
178 molds. Paste is poured in 3 times with 30 s of vibration on a vibrating table between each
179 pouring to ensure the maximum removing of air bubbles within the sample. Bottles are
180 hermetically sealed and samples were cured for 3 days in dark tanks, at a 25°C temperature
181 and relative humidity greater than 90%.

182 2.3. *Color analysis*

183 The blue-green color of GGBFS-containing materials is a key parameter in this study.
184 However, visual color determination is not objective and greatly varies between individuals.
185 A portable spectrophotometer Konica Minolta CM-700d objectively determined the color of

186 formulated samples, working in the L*a*b* (or CIELAB) color space and following the NF
187 EN ISO/CIE 11664-4 (07/2019) standard. The measure used 3 parameters to quantify a color:
188 one for the brightness (L*), and two for axis of opposite colors (a* and b*). The L* parameter
189 ranges from the darkest (-100) to the brightest (+100), the a* parameter ranges from green (-
190 60) to red (+60), and the b* parameter ranges from blue (-60) to yellow (+60).

191 The coloration measurements were conducted for all concrete and cement/GGBFS samples
192 just after demolding. At least 3 different points were analyzed on the face of the samples in
193 contact with the bottom of the molds ('bottom face'), and 5 points on the larger curved side
194 ('side face'). Values were averaged for each side of each samples.

195 *2.4. Tank Monolith Leaching test*

196 The common and well-known tank monolith leaching test was chosen to mimic a green fair-
197 faced concrete washed by flowing or surrounding water, in line with the recommendations to
198 evaluate materials close to the effective real conditions (van der Sloot 2000). This test is
199 presumed to be quite representative of real scenario since GGBFS-rich cements are often
200 employed in wet aggressive environments, in particular in presence of sulfates or chlorides
201 (Osborne 1999). In these conditions, concrete can be subjected to leaching by infiltrated rain
202 water, or by flooding with groundwater or surface water. The tank monolith test used in the
203 present study followed the XP CEN/TS 15862 (10/2012) standard. A solid monolith has been
204 immersed in deionized water for 24 h, in a single batch and without water renewal. The ratio
205 of Liquid on exposed solid surface Area (L/A) was defined to 12 cm³/cm² for all samples.
206 Average dimensions were of 7.2 cm diameter for 12.5 cm height. A minimal thickness of 2
207 cm of the water layer around the sample has to be observed, to facilitate a proper leaching on
208 every faces. Thus, samples were put on a HDPE mesh disposed at the bottom of a 5 L HDPE
209 container. Homogenization of the solution was ensured with a magnetic stirrer during the test.

210 2.5. Leachates analysis

211 Leachates were filtrated through a 0.45 μm pore size cellulose acetate filter. Four subsamples
212 were created: the first for pH and conductivity measurement with a Knick Portavo® 907
213 Multi portable multimeter, the second subsample for anions analysis, the third subsample was
214 mixed with SAOB solution for sulfides analysis, and the fourth was acidified with 2 mL
215 HNO_3 65% analytical grade (Merck) for element analysis.

216 Chlorides and sulfur species were the analyzed anions. Sulfates SO_4^{2-} , thiosulfates $\text{S}_2\text{O}_3^{2-}$ and
217 sulfides S^{2-} have been regularly reported into GGBFS-containing materials effluents (Glasser
218 et al. 1988; Gruskovnjak et al. 2006; Lothenbach et al. 2011). This is not surprising
219 considering that sulfur is on an average concentration of 1.27 wt.% in Fe-slag (which includes
220 BFS and steel slags), ranging from 0.38 to 3.15 wt.% (Piatak et al. 2015), with sulfur being
221 predominantly under the reduced sulfide form (Glasser et al. 1988). In the alkaline and mildly
222 reductive environment at work in leachates of GGBFS-containing materials, these sulfur
223 species are in a close thermodynamically stable range (Pourbaix and Pourbaix 1992). Anions
224 analysis was performed by ion chromatography. Subsample was filtrated a second time on
225 0.22 μm Sartorius filter, before being stored at 4°C in the dark. The Metrohm 882 Compact
226 ion chromatography was equipped with a Metrosep A Supp 5 Guard/4.0 precolumn (5 x 4.0
227 mm) and a Metrosep A Supp 4 column (250 x 4.0 mm). The conductimetric detection was
228 enhanced with a chemical suppressor. A mobile phase constituted of a 1.8 mM Na_2CO_3 and
229 1.7 mM NaHCO_3 mix, with 2% acetone, was used at a $1\text{mL}\cdot\text{min}^{-1}$ flow rate with 20 μL of
230 injection volume. Calibration was made with standard solutions, prepared with commercial
231 certified Alfa Aesar multi-anions 1000 $\text{mg}\cdot\text{L}^{-1}$ (ref 041693) solution.

232 For sulfide analysis, the third subsample was mixed with SAOB solution at a 1:1 ratio into 50
233 mL polypropylene (PP) tubes, in a way to minimize the gas headspace. A modified USEPA

234 method 9215 (12/1996) was used to carry out sulfides analysis. Analyses were conducted in
235 the same way that solution coming from the acid distillation of solid samples to analyze
236 sulfides content (cf. section II.1).

237 The fourth acidified subsample was used for major and minor element analyses (Si, Al, Fe,
238 Mn, Mg, Ca, Na, K, Cr) by ICP-OES (Thermo Scientific iCAP 6500) and Atomic Absorption
239 Spectroscopy (Varian AA240FS).

240 *2.6. Ecotoxicological assessment*

241 *2.6.1. Microalgae: growth inhibition assay*

242 The green microalgal species used for the test was *Raphidocelis subcapitata* (SAG 61.81).
243 Briefly, six different replicates were conducted for each concentration, using a 96-well
244 microplate according to ISO 8692 (2012) guideline. Wells are completely filled with solution
245 and covered hermetically. Zinc (prepared from ZnSO₄) was used as positive control. The algal
246 culture in the exponential growth phase was diluted in ISO medium for freshwater algae (pH
247 8.1 ± 0.2) to obtain an inoculum for the test with a cell density of 20,000 cells.mL⁻¹ and the
248 recommended dose of nutrients in exposure medium. As initial pH of leachates was very
249 high, pH has been considered as potential confounding factor. Thus ecotoxicity assessment
250 was led at initial pH and at adjusted value of pH 8.10. The test plates were incubated in a
251 room with continuous illumination of 100 μmol.m⁻².s⁻¹ (cool-white fluorescent lamps) at 23 ±
252 2°C. After 72 h of incubation at 23 ± 2°C, the fluorescence variation was measured at
253 wavelength of 485 nm for excitation and 640 nm for emission with VICTOR Nivo multimode
254 plate reader (PerkinElmer). EC50 were determined by using Regtox macro and results were
255 presented in TU (Toxic Unit = 100/EC50).

256 2.6.2. *Microcrustacea: immobilization assay*

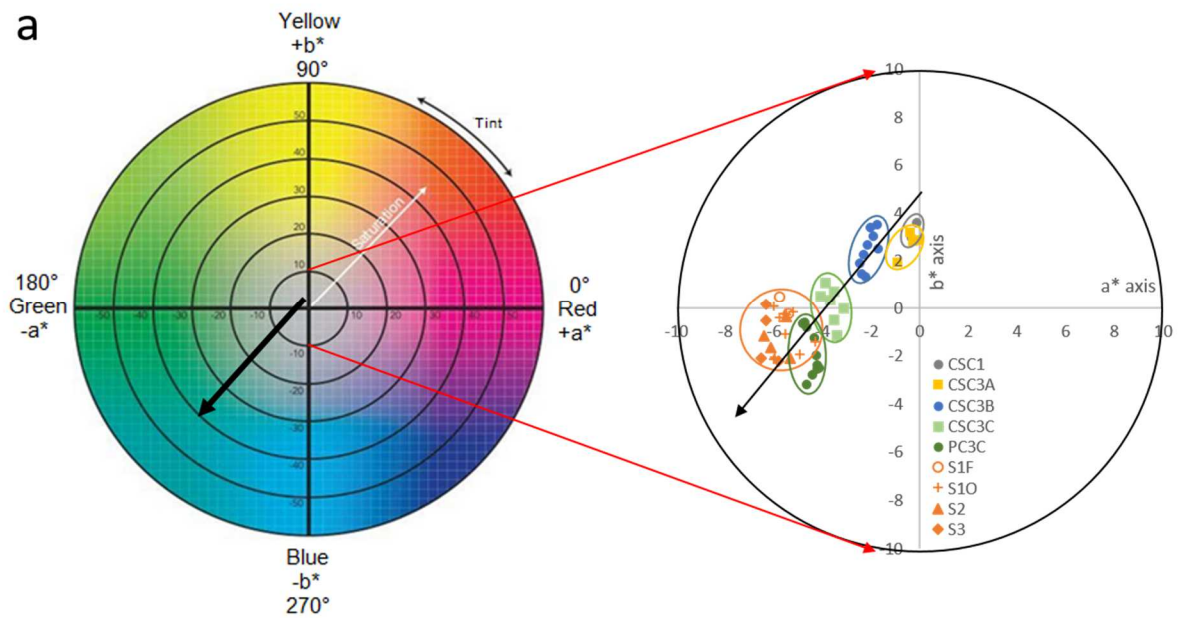
257 The microcrustacean immobilization assay was performed according to ISO 6341 (2012).
258 Three different experiments (with four replicates/tubes for each one) were performed. An
259 assay tube with 10 mL of culture medium (pH 7.8 ± 0.5 , aerated overnight) plus the
260 appropriate concentration of leachate was prepared for each replicate. Tubes are completely
261 filled with solution and covered hermetically. Leachates were tested at initial pH and at
262 adjusted value of pH 8.10. Five young *D. magna* (up to 24 hours of life) were then added to
263 each tube. Potassium dichromate was used as positive control. The test tubes were covered
264 with aluminum foil to keep light out and were kept in an incubator at $20 \pm 2^\circ\text{C}$. Inhibition of
265 the mobility of the individual *D. magna* was determined visually after 48 h of exposure. EC50
266 were determined by using Regtox macro and results were presented in TU (Toxic Unit =
267 $100/\text{EC50}$).

268 3. Results and discussion

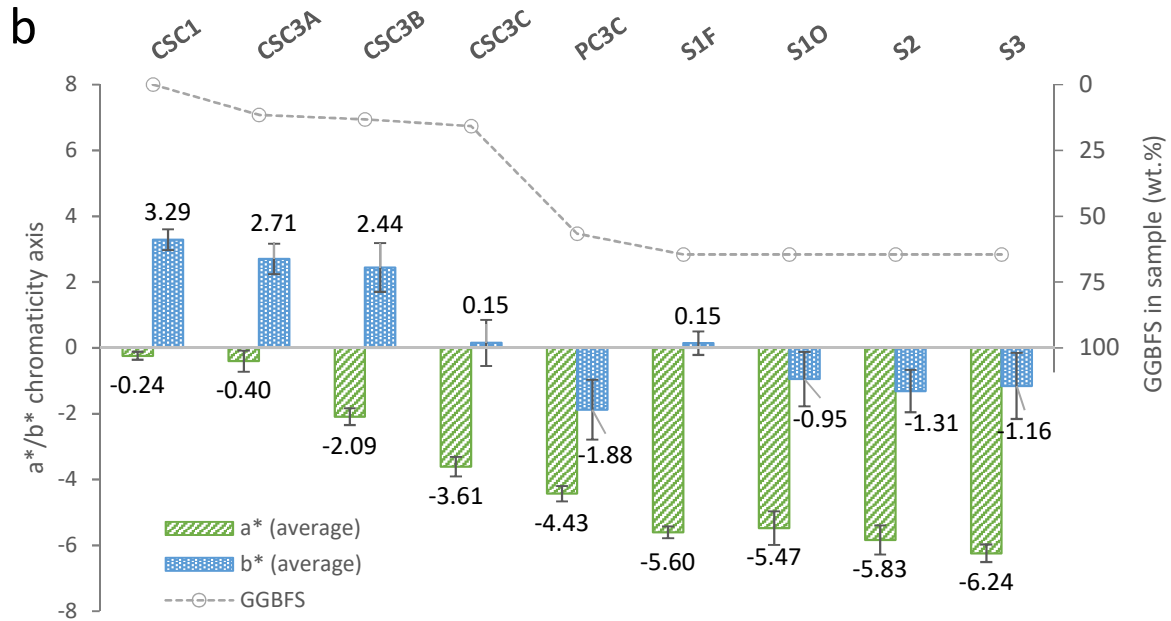
269 3.1. *Color evaluation of GGBFS-containing materials*

270 The color was evaluated immediately after demolding. The first result emerging from these
271 measurements is the overall green-blue color borne by all samples, with a clear evolution
272 towards the green-blue quadrant of the circle, as showed by the black arrow (Fig. 1a). The a^*
273 parameter has a maximum of -0.24 for CSC1 and a minimum of -6.24 for the S3 GGBFS
274 (Fig. 1b). This parameter evolves quite linearly with the GGBFS content ($R^2 = 0.876$), with a^*
275 decreasing while GGBFS content heightened, meaning color is moving towards the green side
276 of the axis. For concrete materials, CSC1 and CSC3A samples have a close value of a^* (-0.24
277 and -0.40 respectively), despite CSC1 has no GGBFS content, and CSC3A having 11.5 wt.%
278 GGBFS in the total material. However, a slight increment of GGBFS in the total material

279 leads to a noticeable raise of the a^* parameter. CSC3B sample has 1.7 wt.% more of GGBFS
 280 than CSC3A (for a total of 13.2 wt.%), with a^* decreasing to -2.09, and CSC3C sample has
 281 4.3 wt.% more of GGBFS than CSC3A (total of 15.8 wt.%) with a^* decreasing to -3.61.
 282 Comparatively, the high increase of GGBFS content for PC3C to 56.7 wt.% doesn't go along
 283 with a steep decrease of a^* , lessening to -4.43. For the four GGBFS pure paste samples, a^*
 284 oscillates between -5.47 and -6.24. The freshness of the GGBFS production does not seem to
 285 influence much the a^* parameter, by comparing a^* value of S1F and S1O.



286



287

288 **Figure 1 (color on web only).** Dispersion of samples on a* and b* axis depicted on the
 289 chromatic circle representing the L*a*b* CIE 1976 color space, modified from
 290 www.colorimax.com (a), and average values for a* and b* parameters and wt.% proportion of
 291 GGBFS in concrete, cement and GGBFS paste samples, with error bars standing for standard
 292 deviation (SD) (b).

293

294 The b* parameter has a maximum of +3.29 for CSC1 sample and a minimum of -1.88 for
 295 PC3C sample. Its evolution is less linear, PC3C having the smallest value while having not
 296 the highest GGBFS content (56.7 wt.% against 64.5 wt.% into GGBFS pure paste). However,
 297 the coefficient of correlation between b* parameter and GGBFS content being $R^2 = 0.774$ still
 298 indicates a positive and noticeable correlation between those two parameters, b* decreasing
 299 while GGBFS content raises, meaning that color of the samples is moving towards the blue
 300 side of the axis. Similarly than for a*, the addition of GGBFS from CSC1 to CSC3A comes
 301 with a slight decrease of b*, from 3.29 to 2.71. However, a discrepancy is observed not
 302 between CSC3B sample and CSC3C sample (b* decreasing from 2.71 to 2.44), but between

303 CSC3B and CSC3C, b^* falling to 0.15, for a +2.6 wt.% increase of GGBFS content. The
304 evolution of samples from concretes to pure paste goes along with a decrease of b^* from 0.15
305 for CSC3C concrete to -1.88 for the PC3C. Then, for the four GGBFS pastes, the b^* value
306 oscillates between 0.15 and -1.31.

307 Nevertheless, this is noticeable that the color of samples is much more spread on the b^* axis
308 than the a^* axis (Fig. 1a). Most of the samples are more scattered vertically on the blue-
309 yellow axis. It seems that the color characterization of GGBFS-containing materials might be
310 more reliable on the a^* component in the $L^*a^*b^*$ color space, and more uncertain on the b^*
311 component.

312 The color investigation of GGBFS samples is generally consistent with the common visual
313 observation made during civil engineering works involving GGBFS-containing concretes.
314 Samples color is tending towards the green-blue color after casting of formwork, color which
315 usually fade away in days. The color of GGBFS pure paste with GGBFS originated from
316 different cast iron production sites seems to have some slight differences, a^* ranging from -
317 5.47 for S10 to -6.24 for S3, and b^* from 0.15 for S1F to -1.31 for S2. Despite these
318 differences, it is difficult to attribute these variations to the different origins of GGBFS,
319 because of the relatively important standard deviation SD, particularly for b^* parameter (SD
320 of b^* ranging from 0.36 to 1.00).

321 *3.2. Leachates chemistry of tank monolith leaching test*

322 A tank monolith leaching test was performed over 24 h for all samples and leachates were
323 characterized immediately after. Concentrations in eluates as mg.L^{-1} (and mmol.L^{-1}) are
324 normalized with the L/A (L.m^{-2}) ratio as mg.m^{-2} (and mmol.m^{-2}).

325 *3.2.1. Metals measurement*

326 The results are given in **Table 2**. Minor elements Fe, Mn and Cr were monitored because of
 327 their hypothetical -but never demonstrated- role in the greening effect. The Fe²⁺ and Cr³⁺ ions
 328 give the green color in silicates minerals like olivine or diopside. In addition, chromium was
 329 also monitored due to its well-known presence in cements and its hazardous behavior when
 330 under chromate form (Cr⁶⁺) towards environment and human health. In the present study no
 331 chromium was found in the leachates, as well as no iron nor manganese, except iron in CSC1
 332 leachates to an amount of 0.06 mmol.m⁻² close to the limit of detection (Table 2). The absence
 333 of chromium in leachates is consistent with the usual utilization of cement (either with
 334 GGBFS or not) for the treatment by stabilization/solidification of hazardous wastes
 335 contaminated with trace metals such as chromium (Paria and Yuet 2006). Considering the
 336 overall highly alkaline conditions at work in concretes and pastes samples, iron and
 337 manganese were not expected to be leached in detectable amounts.

338 **Table 2.** Concentrations of major and minor elements elements in the leachates of the tank
 339 monolith leaching test

	Na	Ca	K	Al	Si	Fe [*]	Mn ^{**}	Cr ^{***}	Ca/Si	Al/Si
	mmol.m ⁻²								-	-
CSC1	80.76	524.19	82.43	1.63	5.48	0.06 ^a	n.d.	n.d.	95.61	0.30
CSC3A	118.24	178.79	45.89	4.92	9.89	n.d.	n.d.	n.d.	18.08	0.50
CSC3B	57.34	172.92	42.80	4.24	11.89	n.d.	n.d.	n.d.	14.55	0.36
CSC3C	35.68	105.37	13.49	5.23	12.90	n.d.	n.d.	n.d.	8.17	0.41
PC3C	38.78	154.48	27.00	8.39	19.61	n.d.	n.d.	n.d.	7.88	0.43
S1F	1861.59	53.23	14.99	15.33	26.81	n.d.	n.d.	n.d.	1.99	0.57
S1O	1893.76	40.26	14.98	13.53	20.83	n.d.	n.d.	n.d.	1.93	0.65
S2	2224.62	36.78	12.51	15.15	25.33	n.d.	n.d.	n.d.	1.45	0.60
S3	1522.16	26.82	9.12	12.43	18.90	n.d.	n.d.	n.d.	1.42	0.66

340 n.d.: not determined. Result is lower than the limit of detection, which prevents from calculating
 341 concentrations as mmol.m⁻²

342 ^a Fe concentration in leachate = 2.9 × 10⁻² mg.L⁻¹

343 * LD(Fe) = 1.0 × 10⁻² mg.L⁻¹

344 ** LD(Mn) = 1.0 × 10⁻³ mg.L⁻¹

345 *** LD(Cr) = 2.0 × 10⁻¹ mg.L⁻¹

346
347 Description: Concentrations of major elements (Na, Ca, K, Al, Si) and minor elements (Fe,
348 Mn, Cr) in leachates of the tank monolith leaching test are given as mmol.m^{-2} . Ca/Si and Al/Si
349 ratio are also displayed.

350 **Major elements**

351 Na, Ca, K, Al and Si were the major elements released in leachates (Table 2). For alkaline
352 metals, potassium is released in samples leachates between 9.12 and 82.43 mmol.m^{-2} . The
353 global trend is a reduction in leachates with the increase of GGBFS. Potassium releases are
354 roughly correlated with the initial potassium content as K_2O ($R^2 = 0.797$) (Table 1), probably
355 also controlled as a very soluble element by diffusion in matrix which porosity decreased with
356 the increased amounts of GGBFS. Sodium is a highly soluble cation quantified in cement-
357 made samples leachates at concentrations between 35.7 and 118.2 mmol.m^{-2} . Sodium
358 concentrations are ten to twenty times higher in GGBFS pure pastes leachates, until 2224
359 mmol.m^{-2} for S2 paste leachates. Such discrepancy is explained by the addition of 5 wt.%
360 NaOH to the initial mix of GGBFS pure pastes to accelerate the setting kinetic.

361 Calcium is the most released element, with exception of sodium in GGBFS pure pastes.
362 Calcium concentrations range between 26.82 mmol.m^{-2} for S3 GGBFS paste and 524.19
363 mmol.m^{-2} for CSC1 concrete, and calcium leaching correlates well with the total
364 concentration as CaO in cement and GGBFS ($R^2 = 0.982$). Aluminum and silicon leaching are
365 also quite correlated to their total oxide contents with respective correlation coefficient of
366 0.637 and 0.766. In leachates, aluminum is analyzed to concentrations between 1.63 mmol.m^{-2}
367 for CSC1 concrete and 15.33 mmol.m^{-2} for S1F paste, and silicon between 5.48 mmol.m^{-2}
368 for CSC1 concrete and 26.81 mmol.m^{-2} for S1F paste.

369 The correlation between major elements leaching and their oxide content is linked to the
370 similar raw composition of cement and BFS, mainly composed of CaO, SiO₂ and Al₂O₃.

371 However, one of the main differences between both is the respective proportion of the oxides.
372 From Table 1 and compared to the four GGBFS, CEM I cement (mainly made of Portland and
373 minor secondary constituents) is richer in CaO (62.91 versus 41.49 – 42.41 wt.%), and
374 depleted in Al₂O₃ (5.44 versus 11.40 – 11.89 wt.%) and SiO₂ (20.69 versus 37.28 – 37.57
375 wt.%). In composite cements, CEM III/A, CEM III/B and CEM III/C, the partial complement
376 of Portland cement by GGBFS from 62 to 85 wt.% modifies the mass proportion of main
377 oxides in the mix. In fact, increasing the GGBFS content heightens the SiO₂ and Al₂O₃
378 content and decreases the CaO content, which is reverberated on the further available
379 elements for the formation of cement hydrates after hydration. Experimentally, the minerals
380 observed in hydrated cement-slag systems are portlandite, C–(A)–S–H, ettringite, Afm and an
381 hydrotalcite-type phase (Lothenbach et al. 2011). In GGBFS high-substituted mix, the lack of
382 available calcium leads to the consumption of portlandite hydrates to supply the precipitation
383 of C–S–H (Kolani et al. 2012). Furthermore, enrichment in Al₂O₃ leads to the greater
384 incorporation of aluminum into C–S–H to form C–A–S–H, as well as increasing other
385 aluminates hydrates (Lothenbach et al. 2011).

386 **Ca/Si and Al/Si ratios**

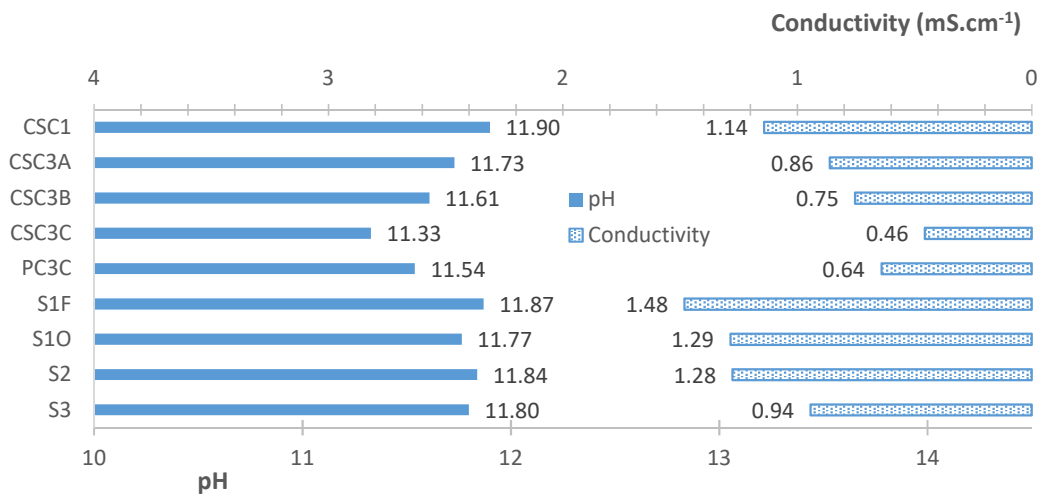
387 Discrepancies in the quantities and composition of hydrates formed during hydration then
388 influence the chemistry of leachates, which is noticeable in the evolution of Ca/Si and Al/Si
389 ratios between all systems (Table 2). Increasing the proportion of GGBFS in the mix leads to
390 a net decrease of the Ca/Si ratio, from 95.61 for CSC1 to 8.17 for CSC3C. For GGBFS pure
391 pastes, Ca/Si ratio oscillates between 1.42 and 1.99. Calcium is less eluted in leachates of
392 GGBFS-containing pastes and concretes mostly because of two alongside mechanisms.
393 Firstly, calcium is less available to leaching solution due to the portlandite consumption by C–
394 S–H. Analyses of CEM I and CEM III/A cement pastes by TGA showed that GGBFS-
395 containing paste contained less than half the portlandite content of CEM I paste (Kamali et al.

396 2008). In addition to ions in interstitial solutions, portlandite is the main source of calcium
397 leaching in cement-based materials, while silicon mainly comes from the incongruent
398 dissolution of C–S–H (Faucon et al. 1996; Müllauer et al. 2015), although depending on the
399 leaching solution C–S–H may also contribute to calcium leaching (Kamali et al. 2008).

400 Secondly, one of the main structural effect of GGBFS addition in cement mix is the reduction
401 of porosity, combined to a more important resistance to ions movement increasing with the
402 decrease of Ca/Si ratio of C–S–H (Luan et al. 2012). In cement-based materials, the transport
403 is controlled by diffusion mechanisms, depending on the porosity (Haga et al. 2005). This
404 porosity effect is particularly seen on sodium leaching. Although CSC3C concrete has a
405 higher Na₂O content with 0.31 wt.% than CSC3B (0.22 wt.%) or CSC1 (0.20 wt.%), only
406 35.68 mmol.m⁻² are leached, versus 57.34 mmol.m⁻² for CSC3B and 80.76 mmol.m⁻² for
407 CSC1, consistently with literature (Müllauer et al. 2015). The Al/Si ratio is heightened with
408 the increase of GGBFS from 0.30 for CSC1 to 0.41 for CSC3C with a higher than expected
409 value of 0.50 for CSC3A. Both aluminates and silicates evolve in the same way with the
410 substitution of Portland cement with GGBFS. In GGBFS pure pastes, Al/Si ratio oscillates in
411 a narrow range between 0.57 and 0.66. Despite GGBFS have a very similar composition
412 regarding main oxides, i.e. Al₂O₃, CaO and SiO₂, it seems that other factors influence the
413 composition of leachates. For example, S1F and S1O leached 53.23 and 40.26 mmol.m⁻² of
414 Ca respectively, or 26.81 and 20.83 mmol.m⁻² of Si. Fresh production seems to be more easily
415 “leachable”. Further investigations should be conducted to evaluate factors that lead to the
416 different leaching behavior observed. In particular, mineralogical investigations should focus
417 on the identification of hydrates formed and their relative proportions. Finally, alkalis Na and
418 K are quickly and easily eluted because of their weak bonding with C–S–H gels (Müllauer et
419 al. 2015).

420 3.2.2. pH and conductivity

421 Overall, the pH measured in leachates of samples is greatly alkaline, with values ranging from
 422 11.33 to 11.90 (Fig. 2). Two trends are identifiable, depending on the materials assessed,
 423 concrete or pure paste. For leachates of concrete samples, pH values are ranging from 11.33
 424 for CSC3C concrete to 11.90 for CSC1 concrete, almost linearly diminishing with the
 425 increased concentration of GGBFS. In leachates of PC3C sample, pH is higher than for
 426 CSC3C with 11.54 units despite GGBFS content increase (56.7 wt.% of the total sample).
 427 However, in concretes the hydraulic binder only represents 18.5 wt.% of the total sample
 428 mass against 66.7 wt.% in cement paste. The pH raise can be linked in this case to the greater
 429 proportion of binder accounting for the total mass of the sample. A second trend is related to
 430 the GGBFS pure paste, pH of which is oscillating between 11.77 and 11.87 units. Compared
 431 to the group of concrete samples, GGBFS pure pastes produce leachates with higher pH, most
 432 probably attributed to the 5 wt.% NaOH addition used for the hydraulic latent setting of
 433 GGBFS. Therefore, GGBFS of different origins conduct to minor pH differences.



434

435 **Figure 2 (color on web only).** pH in leachates (blue plain bars) and conductivity (blue dotted
436 bars) of leachates from concretes, cement paste and GGBFS pure pastes after having been
437 subjected to the tank monolith leaching test

438 Conductivity of the leachates ranges from 0.46 mS.cm^{-1} to 1.48 mS.cm^{-1} (Fig. 2). As well as
439 for pH results, a trend is clearly visible for leachates of concrete samples, with a sharp drop
440 from 1.14 mS.cm^{-1} for CSC1 to 0.46 mS.cm^{-1} for CSC3C. Thus, conductivity decrease is well
441 correlated to the increase of GGBFS content in the four concrete samples ($R^2 = 0.849$).

442 Conductivity for leachate of cement paste PC3C is higher than for CSC3C concrete (0.64
443 versus 0.46 mS.cm^{-1}), most probably because of the lack of aggregates and the simultaneous
444 augmentation of the relative fraction of binder. However, unlike pH results, conductivity of
445 leachates of GGBFS pure paste shows some discrepancies. In particular, despite the very
446 close chemical composition of the four pastes (Table 1), conductivity ranges from 0.94
447 mS.cm^{-1} for S3 sample to 1.48 mS.cm^{-1} for S1F sample (Fig. 2). For the four GGBFS, XRF
448 results show that Al_2O_3 ranges between 11.20 and 11.89 wt.%, CaO between 41.49 and 42.41
449 wt.% and SiO_2 between 37.28 and 37.57 wt.%, for the main components of GGBFS employed
450 to make pure pastes (Table 1).

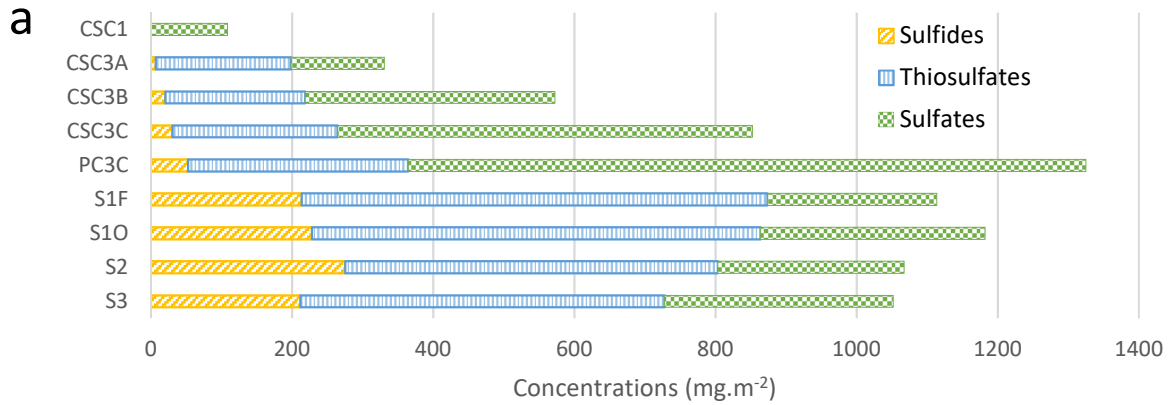
451 **Relation with cement hydrates**

452 In cement-based materials, portlandite dissolution is responsible for the alkaline pH available
453 in interstitial water. The replacement of Portland cement by GGBFS, and the global increase
454 of GGBFS in a cement mix, induces a reduction in the CaO total content. Thereby, such
455 hydrated systems are deficient regarding to portlandite, leading to a lower pH in interstitial
456 water. In addition to the lesser portlandite precipitated, pH is reduced concomitantly in
457 GGBFS highly substituted systems by the competition of soluble sulfur species negatively
458 charged in pore water with dissolved hydroxides ions to conserve electro-neutrality of the
459 solution (Gruskovnjak et al. 2006; Lothenbach et al. 2011). In leachates, pH is lower for

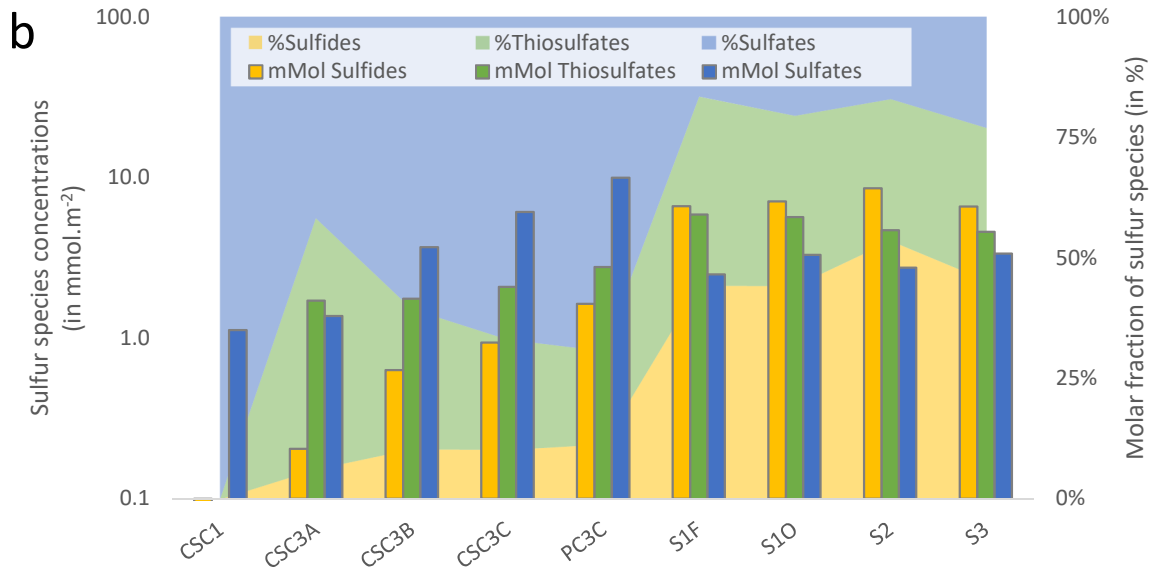
460 highly substituted systems, as well as calcium leaching compared to a CSC1 concrete (Table
461 2). Concomitantly to the availability of soluble species and elements such as $\text{Ca}(\text{OH})_2$,
462 porosity and potential resistance to ions movement created by the morphological differences
463 of precipitated hydrates (in particular C–S–H becoming 2D-shaped when Ca/Si ratio
464 decreases) may also affect pH and conductivity in the same way it affects leaching of
465 elements by reducing the potential mobility in a diffusion-controlled system (Table 2). Then,
466 the lower permeability of GGBFS high-substituted systems will lessen the release of major
467 elements (Na, Ca, K) as well as hydroxide ions, except in GGBFS pure pastes where Na is
468 highly concentrated due to the use of NaOH as activator and leached in important quantities
469 ($1800 - 2200 \text{ mmol.m}^{-2}$), leading to higher than expected conductivities.

470 3.2.3. Sulfur chemistry

471 Sulfur anions (sulfides, thiosulfates, sulfates) have been quantified into the leachates of
472 samples subjected to the tank monolith leaching test (Fig. 3). Sulfates are leached by all
473 samples, between 108 mg.m^{-2} for CSC1 sample and 960 mg.m^{-2} for PC3C (Fig. 3a).
474 Thiosulfates are released by all samples, except for CSC1, between 192 and 660 mg.m^{-2} , as
475 well as sulfides which are released between 6.6 and 275 mg.m^{-2} . Sulfates ions represent 17.1
476 to 100.0% of the molar fraction of the three analyzed sulfur anions (Fig. 3b). Sulfates ions are
477 the major ion released in CSC1 (100.0%), CSC3B (60.6%), CSC3C (66.9%) and PC3C
478 (69.3%) leachates, whereas thiosulfates represent 52.0% in CSC3A leachates versus 41.7%
479 for sulfates. For GGBFS pure pastes, sulfides are the major ion released, representing from
480 44.2 to 53.5% of the total molar fraction of sulfur anions. Then, thiosulfates account for 29.4
481 to 39.1% , with sulfates being the minor ion.



482



483

484 **Figure 3 (color on web only).** Mass concentration of anions sulfides S^{2-} , thiosulfates $S_2O_3^{2-}$,
 485 and sulfates SO_4^{2-} (as $mg.m^{-2}$) (a), molar concentration and respective molar proportions of
 486 each anions as a percent of total sulfur anions analyzed (b) in leachates of concretes, cement
 487 paste, and GGBFS pure pastes subjected to the tank monolith leaching test.

488 **Concretes and CEM III/C cement paste**

489 In absolute value, the three sulfur anions are increasingly released when GGBFS substitution
 490 increase in the leachates of the four concretes. More generally, evolution of sulfur anions
 491 releases between the four concretes and the cement paste follows a similar pattern for sulfides
 492 and sulfates, substantial enrichment between CSC3A and CSC3B (almost triple), and then
 493 +50 to +75% between CSC3B and CSC3C, and CSC3C and PC3C respectively. On the

494 contrary, thiosulfates releases are almost stable around $200 \text{ mg}\cdot\text{m}^{-2}$ at the same time (Fig. 3a).
495 Sulfides, missing for CSC1, appear in CSC3A leachates with $6.6 \text{ mg}\cdot\text{m}^{-2}$, and increase to 20.3
496 $\text{mg}\cdot\text{m}^{-2}$ for CSC3B, and $30.1 \text{ mg}/\text{m}^2$ for CSC3C. For PC3C, sulfides and sulfates
497 concentrations are almost doubled, but not thiosulfates.

498 Sulfates as a major release in leachates of concretes and cement paste is not surprising, since
499 cements include setting time regulators e.g. gypsum or anhydrite which readily precipitate
500 with aluminates to form ettringite (Aft) and monosulfoaluminate (Afm). Still, sulfides are
501 released in concrete leachates in far from negligible amounts, accounting for 6 to 10% of the
502 molar fraction in concretes leachates, that is to say from 6.6 to $30.1 \text{ mg}\cdot\text{m}^{-2}$ in term of mass
503 (Fig 3a, 3b). This result can be expected, considering that GGBFS included into CEM III
504 cements bring sulfides ions, for a total between 0.55 and 0.74 wt.% in the three CEM III
505 cements.

506 **Origin of reduced sulfur anions**

507 GGBFS is actually a rather reducing material than Portland cement, and redox potential in
508 cement mix with high proportion of GGBFS is able to reach -250 to -350 mV (versus
509 Calomel) (Angus and Glasser 1985; Macphee et al. 1988). Such reducing environment leads
510 to reduced form of sulfur, mostly as amorphous sulfides (Glasser et al. 1988; Roy 2009).
511 Although most of the sulfides ions solubilized in pore water are precipitated with hydrates in
512 early hours after mixing, these species are then gradually released in interstitial solutions
513 (Vernet 1982). The early precipitation of sulfides with first hydrates created when GGBFS is
514 hydrated is probably at the origin of the greening effect (Vernet 1982; Le Cornec et al. 2017).
515 In pore solution, sulfides are oxidized with available dissolved molecular oxygen, leading to
516 main oxidation products, thiosulfates and sulfates (Glasser et al. 1988; Gruskovnjak et al.
517 2006; Lothenbach et al. 2011). However, narrow porosity of cement-based materials limit the
518 oxygen diffusion, hence sulfides ions are partly preserved from oxidation. When samples are

519 submitted to leaching, sulfur anions are released in the leachates from interstitial solution.

520 Sulfides, being the most sensitive to oxidation by molecular oxygen, might be oxidized during

521 the leaching process, depending on the oxygen diffusion in leaching solution.

522 In concretes leachates, the difference between sulfates and sulfides releases is noticeable.

523 Considering molar concentrations, the ratio between sulfates and sulfides releases is overall

524 constant in concretes leachates (except CSC1), and roughly oscillates around 6. Although

525 sulfates are released at lower concentration in CSC1 leachates, it is difficult to conclude on

526 the effective impact of GGBFS on sulfate leaching because of the variable additions of

527 gypsum or anhydrite in cement mix. Whether gypsum or anhydrite, sulfates in cement mix

528 precipitate with aluminates to form Afm and Aft hydrates, further remobilized by leaching

529 solution through surface dissolution, explaining sulfates releases for cement-based samples

530 (Müllauer et al. 2015). A good agreement can be found between quantities of secondary

531 constituents added to cement clinker, and sulfates releases, with 1.12 and 1.37 mmol.m⁻² in

532 CSC1 and CSC3A, and 3.69 and 6.12 mmol.m⁻² in CSC3B and CSC3C (Fig. 3b).

533 On the contrary, thiosulfates presence cannot be explained by the dissolution of a pre-existent

534 mineral specie. Consequently, thiosulfates have only two way of production: either by

535 oxidation of sulfides included in GGBFS, or by reduction of sulfates. However, sulfate

536 reduction is highly unlikely to happen in aerated environment without a microbial mediation

537 (Pourbaix and Pourbaix 1992; Miao et al. 2012). On the other hand, sulfides are very sensitive

538 to oxidation in aerated water, in particular in alkaline solution with pH higher than 11.5 (Kuhn

539 et al. 1983). In concretes leachates, thiosulfates releases are almost in the same order of

540 magnitude than sulfides in terms of molar concentrations (Fig. 3b). The thiosulfates to

541 sulfides molar ratio is about 8.3 in CSC3A leachates, and quickly decrease to 2.8 in CSC3B,

542 2.2 in CSC3C, and 1.7 in PC3C. Else, if the oxidation of sulfides to sulfates is

543 thermodynamically favored, it has been kinetically observed that the oxidation of sulfides by

544 molecular oxygen leads to thiosulfates as the main products, when pH is alkaline, i.e. pH >
545 8.5 (O'Brien and Birkner 1977; Kleinjan et al. 2005). In such pH–Eh conditions, thiosulfates
546 are stable for weeks, and tend to accumulate, with low oxidation to the final product, sulfates.
547 Therefore, only a minor part of the sulfates production in leachates is likely to come from
548 sulfides oxidation.

549 **GGBFS pure pastes**

550 In GGBFS pure pastes, sulfides releases are much more important than in the PC3C cement
551 paste, with values between 211 and 275 mg.m⁻². Sulfates are in the same order of magnitude,
552 being released in leachates with values between 240 and 324 mg.m⁻². Thiosulfates amounts
553 are much more important in GGBFS pastes leachates, ranging from 516 to 660 mg.m⁻². In
554 GGBFS pastes, no source of sulfates are added, and all sulfur species recovered in leachates
555 come from the slag itself. Considering the molar ratio, the sulfates to sulfides ratio is about
556 0.3 – 0.5, the thiosulfates to sulfides ratio is about 0.5 – 0.9, and the thiosulfates to sulfates
557 ratio is about 1.4 – 2.4. Then, it can be firstly concluded that the amounts of sulfides observed
558 into leachates are in good agreement with both sulfates and thiosulfates releases, and secondly
559 that as stated in literature, thiosulfates represent the main oxidation products in alkaline
560 solutions, but not the only one (O'Brien and Birkner 1977; Kleinjan et al. 2005).

561 *3.3. Ecotoxicological assessment of leachates*

562 A positive control solution containing increasing concentrations of zinc (Zn²⁺) was tested for
563 both ecotoxicity assays. In these cases, an appropriate concentration-response curve was
564 observed and the EC₅₀ was determined as 0.017 ± 0.004 mg.L⁻¹ for algae, and 1.96 ± 0.18
565 mg.L⁻¹ for daphnids. These values were according to validity criteria of ISO standards of the
566 both ecotoxicity tests.

567 The results obtained by performing *R. subcapitata* growth rate and *D. magna* mobility tests
 568 are displayed in **Table 3**: in a general way, leachates induced very low ecotoxic effects on
 569 aquatic organisms, as the maximum value did not exceed 5 TU (toxic units). There was no
 570 statistical difference (ANOVA followed by Tukey test) between data obtained with CEM I
 571 cement, used as a comparison reference, and CEM III/B cement, mainly constituted from
 572 GGBFS (71% cf. Table 1) and clinker. Nevertheless, for daphnia, it is noteworthy that
 573 ecotoxic effects were more important when pH was high (pH = 12.5), compared with adjusted
 574 pH of 8.1. In the Toxicity Classification System, a compound with TU between 1.0 and 10.0
 575 is classified in Class III, meaning potentially low acute toxicity (Persoone et al. 2003). Both
 576 CSC1 and green CSC3B leaching samples, for both adjusted and natural pH, are classified as
 577 Class III towards *D. magna* and *R. subcapitata*.

578 **Table 3.** Ecotoxicological results for CSC1 and green CSC3B concretes leachates

Materials	pH	<i>Raphidocelis subcapitata</i> (24h)		<i>Daphnia magna</i> (24h)		<i>Daphnia Magna</i> (48h)	
		EC50 % of leachate	TU	EC50 % of leachate	TU	EC50 % of leachate	TU
CSC1	8.10	33.35	3.00	84.06	1.19	72.30	1.38
CSC1	12.50	31.30	3.19	21.91	4.56	19.60	5.10
CSC3B	8.10	20.62	4.85	64.82	1.54	47.31	2.11
CSC3B	12.10	20.16	4.96	41.85	2.39	39.95	2.50

579 EC₅₀ = half maximal effective concentration; TU = Toxic Units

580 Description: Eluates of Tank monolith leaching test of CSC1 (reference, CEM I cement) and
 581 green CSC3B concretes samples are subjected to growth inhibition assay (*Raphidocelis*
 582 *subcapitata*) to assess chronic toxicity, and immobilization assay (*Daphnia magna*) to assess
 583 acute toxicity. Results are given as EC50 (in % of leachate in the solution) and Toxic Units
 584 (TU).

585 From a general point of view, not much data are available on the ecotoxicity of usual
586 construction materials (Kobetičová and Černý 2017). Considering the physicochemical
587 characteristics of Ordinary Portland Cement (OPC) concretes, there is no objective reason to
588 consider it as ecotoxic, since OPC does not release detectable concentrations of toxic trace
589 metals (Hillier et al. 1999). Incidentally, leaching of OPC pastes does not show phytotoxicity
590 (Märkl et al. 2017). When OPC concrete is used as recycled aggregates, TU are up to 6.8 at
591 48h to *D. magna*, close to our result for CSC1 of 5.10 TU at 48h (Rodrigues et al. 2020).

592 **Impact of pH on ecotoxicity**

593 When GGBFS is added, ecotoxicity is lowered towards *D. magna* test at initial pHs (12.50 for
594 CSC1 against 12.10 for CSC3B), but slightly increased at adjusted pH of 8.10. In fact, pH is a
595 factor that can explain a potential acute toxicity, in particular for sensitive living organisms
596 such as *D. magna*. And the addition of GGBFS usually decreases pH. Either at 24h or 48h, the
597 increase of pH also heightens the acute toxicity: for CSC1, with pH increasing from 8.10 to
598 12.50 (natural pH of leachates), TU increased from 1.19 to 4.56 in 24h and from 1.38 to 5.10
599 in 48h (Table 3). For CSC3B, pH increasing from 8.10 to 12.10 (natural pH of leachates)
600 induced an increase in TU from 1.54 to 2.39 in 24h, and from 2.11 to 2.50 in 48h. Results
601 show the very low sensibility of *R. subcapitata* to pH effect, with a negligible increase of
602 +0.19 for CSC1 and +0.11 for CSC3B. Other studies show that at alkaline pH of 12 produced
603 by cement system such as OPC, daphnia can be entirely immobilized (Choi et al. 2013). The
604 addition of GGBFS can induce a higher ecotoxicity, up to 17.67 TU, but with pH lowered to
605 8-9, this ecotoxicity is reduced to about 2. Effect of pH on *D. magna* is also observed after
606 48h on sewage sludge combustion ashes, with TU ranging from < 1.1 to 10.0 for pH between
607 8.0 and 11.3 (Lapa et al. 2007).

608 **Impact of sulfides on ecotoxicity**

609 Apart from pH, cations and anions are likely to represent a harm to living organisms, but only
610 if they are bioavailable. Bioavailability highly depends on physical and chemical parameters,
611 and in the case of the leaching of a solid material, it mainly depends on particle size
612 distribution, porosity, wet/drying cycles, storage conditions, hydrophobicity (Kobetičová and
613 Černý 2017). In the case of leaching of GGBFS cement-based materials, the only potentially
614 harmful analyte detected is sulfide ion. From the adjusted pH of 8.1 to the natural pH of
615 eluates, sulfides are highly available as they are under HS⁻ or S²⁻ soluble form (Pourbaix and
616 Pourbaix 1992). Since *R. subcapitata* is little sensitive to pH, sulfides could explain the
617 slightly higher ecotoxicity observed with both pH, and in the same way the slightly higher
618 ecotoxicity for *D. magna* assay at adjusted pH (Table 3). In the case of natural pH, *D. magna*
619 being highly sensitive to pH, in particular in such extreme conditions, the higher ecotoxicity
620 observed for CSC1 may rather be attributed to the higher pH. In fact, *D. magna* has been
621 proven as a highly sensitive organism towards sulfides, as well as many freshwater and
622 marine invertebrates (Wang and Chapman 1999; Küster et al. 2005). For lower trophic levels,
623 sulfides impact is variable. Marine bacteria are diversely affected, with growth rate modified
624 or interrupted (Mirzoyan and Schreier 2014), or microalgae's photosynthesis disrupted and
625 viability lowered (González-Camejo et al. 2017). Although, sulfide ion may play a more
626 subtle role in natural water and environment since it has been recognized to reduce the
627 toxicity caused by available metal by binding with them and reducing their bioavailability to
628 organisms such as *D. magna* (Bianchini et al. 2002).

629 More generally, and in another field, blast-furnace and steel-making slags have also been
630 evaluated as potentially suitable for an environmental amendment use (with dilution to limit
631 alkaline pH effects), showing low ecotoxicity of their leaching assessed by microalgae
632 *Chlorella sp.*, cladocerans *Ceriodaphnia dubia*, and bacteria *Vibrio fischeri* (Wendling et al.
633 2013). Analysis of the composition of GGBFS concretes leachates has led to the conclusion

634 that they are very similar to those of OPC leachates, and are thereby safe environmentally
635 (Parron-Rubio et al. 2019). All these results should lead to the conclusion that the use of
636 GGBFS, whether as construction material in civil engineering or other fields, does not
637 represent a threat to the environment, including the greening effect whatever it is originated
638 from. Two major points have been highlighted, the alkaline pH and the release of sulfides
639 ions. For alkaline pH, GGBFS lowers the pH in concretes compared to OPC, which can only
640 be an improvement towards the receiving environments. Regarding the sulfides release, they
641 can be a minor ecotoxic threat to living organisms. However, sulfides are very sensitive to
642 oxidation by molecular oxygen, especially around natural pH of 7.0–8.0. Under pH 8, sulfides
643 equilibrium is displaced towards H₂S which is a low soluble specie in water, and hydrogen
644 sulfide evaporates being then diluted and oxidized in ambient air. Further investigations
645 should be conducted on the aging of cement-based materials containing GGBFS, including
646 the assessment of the ecotoxicological impact.

647 4. Conclusions

- 648 - The temporary greening effect of GGBFS-containing materials has no particular
649 impact neither on the chemistry of leachates, nor ecotoxicity.
- 650 - The alkaline pH, usually around 11–12.5, is the main issue with cement-based
651 materials in general, but in real conditions eluates are usually quickly buffered by
652 carbonation or diluted in the soil or running water.
- 653 - High pH may impact the most sensitive organisms, such as the crustacean *Daphnia*
654 *magna* much more sensitive to extreme pH than the algae *Raphidocelis subcapitata*.
- 655 - GGBFS contains noticeable amounts of sulfides easily released when GGBFS-
656 concretes are leached. Very slight ecotoxic effects attributed to sulfides are observed

657 for *D. magna* and *R. subcapitata* (0.7 to 1.85 TU of differences between reference and
658 green concrete samples).
659 - Sulfides being highly sensitive to oxidation by molecular oxygen, sulfides released in
660 solution will quickly be neutralized in environment by oxidation, or by evaporation
661 with pH lowering.

662 5. Acknowledgement

663 The authors are thankful to the SARM laboratory (CRPG, Vandoeuvre-lès-Nancy, France) for
664 its contribution to the element analysis, and to the LCPME laboratory (Villers-lès-Nancy,
665 France) for its contribution to the leachates analysis of sulfur anions. The authors are also
666 particularly grateful for the funding of the study from the ATILH professional association
667 (Paris-La-Defense, France) under reference PRA/12-03, and especially Horacio Colina for
668 offering constant support throughout the project. Finally, the authors use vector parts designed
669 by macrovector (from Freepik.com) for the graphical abstract and acknowledge them for they
670 work.

671 6. Reference list

672 Angus MJ, Glasser FP. 1985. The chemical environment in cement matrices. MRS Online
673 Proceedings Library Archive. 50. doi:10.1557/PROC-50-547

674 Bandow N, Gartiser S, Ilvonen O, Schoknecht U. 2018. Evaluation of the impact of
675 construction products on the environment by leaching of possibly hazardous substances.
676 Environ Sci Eur. 30(1):14. doi:10.1186/s12302-018-0144-2.

677 Bianchini A, Bowles KC, Brauner CJ, Gorsuch JW, Kramer JR, Wood CM. 2002. Evaluation
678 of the effect of reactive sulfide on the acute toxicity of silver (I) to *Daphnia magna*. Part 2:
679 Toxicity results. Environ Toxicol Chem. 21(6):1294–1300. doi:10.1002/etc.5620210626.

680 Chivers T, Elder PJW. 2013. Ubiquitous trisulfur radical anion: fundamentals and
681 applications in materials science, electrochemistry, analytical chemistry and geochemistry.
682 Chem Soc Rev. 42(14):5996–6005. doi:10.1039/C3CS60119F.

683 Choi JB, Bae SM, Shin TY, Ahn KY, Woo SD. 2013. Evaluation of *Daphnia magna* for the
684 Ecotoxicity Assessment of Alkali Leachate from Concrete. Int J Indust Entomol. 26(1):41–46.
685 doi:10.7852/ijie.2013.26.1.041

686 Faucon P, Le Bescop P, Adenot F, Bonville P, Jacquinet JF, Pineau F, Felix B. 1996.
687 Leaching of cement: Study of the surface layer. Cement Concrete Res. 26(11):1707–1715.
688 doi:10.1016/S0008-8846(96)00157-3.

689 Glasser FP, Luke K, Angus MJ. 1988. Modification of cement pore fluid compositions by
690 pozzolanic additives. Cement Concrete Res. 18(2):165–178. doi:10.1016/0008-
691 8846(88)90001-4.

692 González-Camejo J, Serna-García R, Viruela A, Pachés M, Durán F, Robles A, Ruano MV,
693 Barat R, Seco A. 2017. Short and long-term experiments on the effect of sulphide on
694 microalgae cultivation in tertiary sewage treatment. Bioresource Technol. 244:15–22.
695 doi:10.1016/j.biortech.2017.07.126.

696 Gruskovnjak A, Lothenbach B, Holzer L, Figi R, Winnefeld F. 2006. Hydration of alkali-
697 activated slag: comparison with ordinary Portland cement. Adv Cem Res. 18(3):119–128.
698 doi:10.1680/adcr.2006.18.3.119

699 Haga K, Sutou S, Hironaga M, Tanaka S, Nagasaki S. 2005. Effects of porosity on leaching of
700 Ca from hardened ordinary Portland cement paste. Cement Concrete Res. 35(9):1764–1775.
701 doi:10.1016/j.cemconres.2004.06.034.

702 Hillier SR, Sangha CM, Plunkett BA, Walden PJ. 1999. Long-term leaching of toxic trace
703 metals from Portland cement concrete. *Cement Concrete Res.* 29(4):515–521.
704 doi:10.1016/S0008-8846(98)00200-2.

705 ISO 6341. 2012. Water quality – determination of the inhibition of the mobility of *Daphnia*
706 magna Straus (Cladocera, Crustacea) – acute toxicity test.

707 ISO 8692. 2012. Water quality – Fresh water algal growth inhibition test with unicellular
708 green algae.

709 Kamali S, Moranville M, Leclercq S. 2008. Material and environmental parameter effects on
710 the leaching of cement pastes: Experiments and modelling. *Cement Concrete Res.* 38(4):575–
711 585. doi:10.1016/j.cemconres.2007.10.009.

712 Kleinjan WE, Keizer A de, Janssen AJH. 2005. Kinetics of the chemical oxidation of
713 polysulfide anions in aqueous solution. *Water Res.* 39(17):4093–4100.
714 doi:10.1016/j.watres.2005.08.006.

715 Kobetičová K, Černý R. 2017. Ecotoxicology of building materials: A critical review of
716 recent studies. *J Clean Prod.* 165:500–508. doi:10.1016/j.jclepro.2017.07.161.

717 Kolani B, Buffo-Lacarrière L, Sellier A, Escadeillas G, Boutillon L, Linger L. 2012.
718 Hydration of slag-blended cements. *Cement Concrete Comp.* 34(9):1009–1018.
719 doi:10.1016/j.cemconcomp.2012.05.007.

720 Kuhn AT, Chana MS, Kelsall GH. 1983. A review of the air oxidation of aqueous sulphide
721 solutions. *J Chem Tech Biot A.* 33(8):406–414. doi:10.1002/jctb.504330804.

722 Küster E, Dorusch F, Altenburger R. 2005. Effects of hydrogen sulfide to *Vibrio fischeri*,
723 *Scenedesmus vacuolatus*, and *Daphnia magna*. *Environ Toxicol Chem.* 24(10):2621–2629.
724 doi:10.1897/04-546R.1.

725 Lapa N, Barbosa R, Lopes MH, Mendes B, Abelha P, Gulyurtlu I, Oliveira JS. 2007.
726 Chemical and ecotoxicological characterization of ashes obtained from sewage sludge
727 combustion in a fluidised-bed reactor. *J Hazard Mater.* 147(1):175–183.
728 doi:10.1016/j.jhazmat.2006.12.064.

729 Le Cornec D, Wang Q, Galois L, Renaudin G, Izoret L, Calas G. 2017. Greening effect in
730 slag cement materials. *Cement Concrete Comp.* 84:93–98.
731 doi:10.1016/j.cemconcomp.2017.08.017.

732 Lothenbach B, Scrivener K, Hooton RD. 2011. Supplementary cementitious materials.
733 *Cement Concrete Res.* 41(12):1244–1256. doi:10.1016/j.cemconres.2010.12.001.

734 Luan Y, Ishida T, Nawa T, Sagawa T. 2012. Enhanced Model and Simulation of Hydration
735 Process of Blast Furnace Slag in Blended Cement. *J Adv Concr Technol.* 10(1):1–13.
736 doi:10.3151/jact.10.1.

737 Macphee DE, Atkins M, Glassar PP. 1988. Phase Development and Pore Solution Chemistry
738 in Ageing Blast Furnace Slag-Portland Cement Blends. *MRS Proceedings.* 127:475.
739 doi:10.1557/PROC-127-475.

740 Märkl V, Pflugmacher S, Stephan DA. 2017. Effect of leached cement paste samples with
741 different superplasticiser content on germination and initial root growth of white mustard
742 (*Sinapis alba*) and cress (*Lepidium sativum*). *Water Air Soil Poll.* 228(3):111.
743 doi:10.1007/s11270-017-3271-2.

744 Miao Z, Brusseau ML, Carroll KC, Carreón-Diazconti C, Johnson B. 2012. Sulfate reduction
745 in groundwater: characterization and applications for remediation. *Environ Geochem Health.*
746 34(4):539–550. doi:10.1007/s10653-011-9423-1.

747 Mirzoyan N, Schreier HJ. 2014. Effect of sulfide on growth of marine bacteria. Arch
748 Microbiol. 196(4):279–287. doi:10.1007/s00203-014-0968-0.

749 Müllauer W, Beddoe RE, Heinz D. 2015. Leaching behaviour of major and trace elements
750 from concrete: Effect of fly ash and GGBS. Cement Concrete Comp. 58:129–139.
751 doi:10.1016/j.cemconcomp.2015.02.002.

752 O’Brien DJ, Birkner FB. 1977. Kinetics of oxygenation of reduced sulfur species in aqueous
753 solution. Environ Sci Technol. 11(12):1114–1120. doi:10.1021/es60135a009.

754 Osborne GJ. 1999. Durability of Portland blast-furnace slag cement concrete. Cement
755 Concrete Comp. 21(1):11-21. doi:10.1016/S0958-9465(98)00032-8

756 Paria S, Yuet PK. 2006. Solidification–stabilization of organic and inorganic contaminants
757 using portland cement: a literature review. Environ Rev. 14(4):217–255. doi:10.1139/a06-
758 004.

759 Parron-Rubio ME, Perez-Garcia F, Gonzalez-Herrera A, Oliveira MJ, Rubio-Cintas MD.
760 2019. Slag Substitution as a Cementing Material in Concrete: Mechanical, Physical and
761 Environmental Properties. Materials. 12(18):2845. doi:10.3390/ma12182845.

762 Persoone G, Marsalek B, Blinova I, Törökne A, Zarina D, Manusadzianas L, Nalecz-Jawecki
763 G, Tofan L, Stepanova N, Tothova L, et al. 2003. A practical and user-friendly toxicity
764 classification system with microbiotests for natural waters and wastewaters. Environ Toxicol.
765 18(6):395–402. doi:10.1002/tox.10141.

766 Piatak NM, Parsons MB, Seal RR. 2015. Characteristics and environmental aspects of slag: A
767 review. Appl Geochem. 57:236–266. doi:10.1016/j.apgeochem.2014.04.009.

768 Pourbaix M, Pourbaix A. 1992. Potential-pH equilibrium diagrams for the system S-H₂O
769 from 25 to 150° C: Influence of access of oxygen in sulphide solutions. *Geochim Cosmochim*
770 *Ac.* 56(8):3157–3178. doi:10.1016/0016-7037(92)90295-T

771 Rodrigues P, Silvestre JD, Flores-Colen I, Viegas CA, Ahmed HH, Kurda R, de Brito J. 2020.
772 Evaluation of the Ecotoxicological Potential of Fly Ash and Recycled Concrete Aggregates
773 Use in Concrete. *Appl Sci.* 10(1):351. doi:10.3390/app10010351.

774 Roy A. 2009. Sulfur speciation in granulated blast furnace slag: An X-ray absorption
775 spectroscopic investigation. *Cement Concrete Res.* 39(8):659–663.
776 doi:10.1016/j.cemconres.2009.05.007.

777 Schwab AP, Hickey J, Hunter J, Banks MK. 2006. Characteristics of Blast Furnace Slag
778 Leachate Produced Under Reduced and Oxidized Conditions. *J Environ Sci Heal A.*
779 41(3):381–395. doi:10.1080/10934520500423527.

780 Sioulas B, Sanjayan JG. 2001. The coloration phenomenon associated with slag blended
781 cements. *Cement Concrete Res.* 31(2):313-320. doi:10.1016/S0008-8846(00)00371-9

782 van der Sloot HA. 2000. Comparison of the characteristic leaching behavior of cements using
783 standard (EN 196-1) cement mortar and an assessment of their long-term environmental
784 behavior in construction products during service life and recycling. *Cement Concrete Res.*
785 30(7):1079–1096. doi:10.1016/S0008-8846(00)00287-8.

786 Steudel R. 2003. Inorganic Polysulfides S_n²⁻ and Radical Anions S_n^{•-}. In: Steudel R (eds).
787 Elemental Sulfur und Sulfur-Rich Compounds II. *Topics in Current Chemistry.* vol 231.
788 Springer, Berlin, Heidelberg. p.127–152. doi:10.1007/b13183

789 Vernet C. 1982. Comportement de l'ion S²⁻ au cours de l'hydratation des ciments riche en
790 laitier (CLK). *Silic Ind.* 47:85–89.

791 Wang F, Chapman PM. 1999. Biological implications of sulfide in sediment—a review
792 focusing on sediment toxicity. *Environ Toxicol Chem.* 18(11):2526–2532.
793 doi:10.1002/etc.5620181120.

794 Wendling LA, Binet MT, Yuan Z, Gissi F, Koppel DJ, Adams MS. 2013. Geochemical and
795 ecotoxicological assessment of iron- and steel-making slags for potential use in environmental
796 applications. *Environ Toxicol Chem.* 32(11):2602–2610. doi:10.1002/etc.2342.

797 Worldsteel Association. 2020. Steel industry co-products. Brussels, Belgium: Worldsteel
798 Association.